ARMY RESEARCH LABORATORY

# Estimates of the Electromagnetic Radiation From Detonation of Conventional Explosives

Jonathan E. Fine

ARL-TR-2447 September 2001

The findings in this report are not to be construed as an official Department of the Army position unless so designated by other authorized documents.

Citation of manufacturer's or trade names does not constitute an official endorsement or approval of the use thereof.

Destroy this report when it is no longer needed. Do not return it to the originator.

**Army Research Laboratory**

Adelphi, MD 20783-1197

**ARL-TR-2447** **September 2001**

# Estimates of the Electromagnetic Radiation From Detonation of Conventional Explosives

Jonathan E. Fine

Sensors and Electron Devices Directorate

# Abstract

An order of magnitude model is presented to estimate radiation from detonation of conventional explosives in an attempt to predict frequency bands and signal levels detected by other investigators. An earlier model describing the radiation generated by explosions has been refined to include the contribution of the heat capacity of the detonation products and the temperature dependence of the concentration of ionized particles. Relationships are established between explosions of uncased Composition B, the radiation frequency bands, and the *E*- and *B*-field amplitudes as a function of detection distance. The model considers the radiation from particles ionized by passage of the shock wave.

A comparison of the calculated radiation with thermal and background noise estimates shows that the radiation is not detectable above the background radiation even for large explosives at close distances. The fact that radiation has been observed indicates either that the assumptions over-simplify the phenomenon or that the primary mechanism of radiation production has been overlooked. Ionized particles exist $10^6$ to $10^8$ times longer than the time to accelerate across the shock wave, during which the particles could produce radiation by some other means. Therefore, it is likely that the model greatly underestimates the quantity of radiation produced.

# Contents

## Figures



## Tables

# 1. Introduction

## 1.1 Background

This work is the result of a U.S. Army Research Laboratory (ARL) technology base program to investigate the causes of electromagnetic radiation from the detonation of conventional explosives in support of future combat systems. The overall program objective was to provide the technology to develop a passive, portable, self-contained unit that can use input from multiple sensors to detect, locate, and identify sources of weapons fire and explosives detonation. An estimate of the radio frequency (RF) radiation from the detonation of conventional explosives is presented here, which updates an earlier ARL model [1].

Previous reports [1–3] have addressed several aspects of the problem. Reference [1] provided an order-of-magnitude model based on the thermal effects of explosive materials in producing ionized particles that generate the radiation. Emphasis was on blast effects that had propagated far from the actual detonation. Reference [2] addressed the problem of RF effects on a projectile fuze as it passed directly through a shaped charge explosion. Emphasis was on effects close to the detonation region, and information was provided about the heat capacity of the detonation products and effects of temperature in the explosive region on the concentration of ionized particles. Reference [3] was a literature survey of previously detected RF energy associated with battlefield munitions [4–12].

This report describes refinements of the model of Reference [1] that include consideration of the contribution of the heat capacity of the detonation products and the temperature effect on the concentration of ionized particles. We estimate the characteristics of the RF emission from a detonation of a bare explosive charge about the size of a mortar projectile.

## 1.2 Summary of Literature Survey

The most prominent results of earlier work are summarized in table 1. Previous investigators detonated explosives including lead azide, RDX (rapidly detonating explosive), Composition B, Tetryl, and trinitrotolul hexogen. Charge sizes from fractions of a gram to 500 tons ($5 \times 10^8$ grams) were reported. Some radiation was from large caliber Navy projectiles, and other radiation was from bare explosives or metal-encased explosives. Observed radiation frequencies were reported from 1 Hz to 1 GHz. Delay times from initiation of the detonation to observation of the radiation ranged from 80 to 600 μs.

Two investigators reported *E*-field values at distances close to the detonation. Takakura [5] reports $4 \times 10^{-4}$ V/m in the frequency band from 6 to 90 MHz at distances of 1m from 0.1 to 0.4 g of lead azide. Using the inverse distance dependence for the radiated *E*-field, we have extrapolated these to

$4 \times 10^{-8}$ V/m at 10 km. Curtis [7] reported $5 \times 10^{-4}$ V/m from 10 g of RDX at a distance of 6.1 m in the frequency range up to 350 Hz. This extrapolates to $3 \times 10^{-7}$ V/m at 10 km.

In most cases, the researchers suggested possible physical mechanisms (see table 1) but presented no analytical model. Modeling is difficult because there may be multiple causes. Furthermore, radiation from tube-launched weapons such as small arms, mortar, and artillery may exhibit radiation that is comparable to bomb or projectile detonations because the tube walls conduct charged particles and concentrate the expanding propellant gases in one direction.

Table 1. Frequency bands observed by investigators reviewed.

| Investigator | Type of explosive used | Amount of explosive used | Delay/ duration of observed signals | Frequency range | Possible cause suggested by authors |
|---|---|---|---|---|---|
| | | Experimental values of frequency ranges | | | |
| Trinks | Tube-launched artillery projectiles | None given | — | 1–100 kHz | Muzzle flash, ionization of gases near muzzle. |
| | | | | 2 MHz–1GHz | Pulses upon impact at target. |
| | | | | 10 MHz–2GHz | Radiation at detonation from "microsparks" caused by charge equalization at detonation. |
| Takakura | Lead azide | 0.1–0.4 g | 80–100 μs delay | 6–90 MHz | Acceleration of electrons ejected by ionization and dipole formation at shock front. |
| Stuart | Large caliber guns | | — | 250 MHz–1 GHz | None given, experimental results only. |
| Curtis | RDX | 10 G | 2-s delay/19 s duration | 0.5–350 Hz | None given, experimental results only. |
| Gorshunov et al | 50/50 trinitrotolul hexogen | 1000–5000 g | — | 3 Hz–20 MHz | Electrical charges generated asymmetrically from scattered electrified detonation products |
| Cook | Composition B | 70–1100 g | — | Below 10 kHz | Gaseous detonation products form a plasma at surface of gas cloud from ionization by passing through earth's electric field. Gas cloud discharges on contact with ground. |

Table 1 (cont'd). Frequency bands observed by investigators reviewed.

| Investigator | Type of explosive used | Amount of explosive used | Delay / duration of observed signals | Frequency range | Possible cause suggested by authors |
|---|---|---|---|---|---|
| | | Experimental values of frequency ranges | | | |
| Wouters | None given | 1,300 g<br>500 ton<br>(= $4.5 \times 10^8$ g) | None explicitly given<br>8-ms duration (1.3 kg)<br>32-ms duration (500 ton) | — | Blast temperature ionizes detonation products and ambient air and produces a plasma. |
| van Lint | Bare spheres to metal-cased bombs | 10–345,000 g (bare spheres to metal-encased bombs) | 100–200-μs delay | 50 MHz–1 GHz | Separation of charge at interface of explosion products and air to form a vertical dipole moment, with asymmetry induced by reflection of shock wave from ground.<br>Electric sparks from explosion products interacting with casing fragments. |
| Andersen and Long | Bare, plaster-encased, and seeded explosives Tetryl, Composition B | 20–1,087 g | 300–600-μs delay | Less than 600 kHz | Detonation ionizes detonation products, which transfer charge by friction to inert casing particles and fragments. |

# 2. Theoretical Model

## 2.1 The Detonation

We present an order-of-magnitude estimate of the electromagnetic radiation from a detonation or explosion. We use the term "explosion" in the sense described by Wilfred Baker [13] as "a process by which a pressure wave of finite amplitude is generated in air by a rapid release of energy. Some widely different types of energy sources can produce such pressure waves and thus be classified as 'explosives' according to our definition...."

"Regardless of the source of the initial finite pressure disturbance, the properties of air as a compressible gas will cause the front of this disturbance to steepen as it passes through the air...until it exhibits nearly discontinuous increases in pressure, density, and temperature. The resulting shock front moves supersonically, faster than sound speed in the air ahead of it. The air particles are also accelerated by the passage of the shock front, producing a net particle velocity in the direction of travel of the front." This report uses the terms "detonation" and "explosion" interchangeably.

The model is used to estimate the frequency bandwidth of the radiation produced and the electric ($E$) and magnetic ($B$) field amplitudes versus distance from the explosion. Results are presented at 10 km from the explosion. The reader can obtain results at other distances by using the formulas that are provided. The model's results are a function of the temperature within an explosive region. We establish this temperature dependence by assuming an idealized detonation model, is shown in figure 1. The assumptions used in the estimate are italicized.

Some of these assumptions are

- *The undetonated projectile occupies a spherical volume defined by radius $r_0$.*
- *The detonation is initiated at t=0 at the center of a spherical explosive charge.*
- *After initiation of the explosion, a detonation wave propagates outward through the explosive charge with a velocity of 10 mm/μs = $10^4$ m/s [14].*
- *At completion of the detonation at $t=t_0$ (3 μs in this example), the detonation wave has expanded to radius $r_0$, and all the undetonated explosive has been converted to detonation products with the release of thermal energy into the volume of radius $r_0$ [1]. We neglect the portion of energy that is converted into kinetic energy of bomb fragments, explosive products, and optical and acoustic radiation.*
- *No expansion occurs for $t<t_0$.*

The temperature of the region with $r < r_0$ at $t = t_0$ is given by

$$T(t_0) = \frac{Q}{C_{V/Det\,\mathrm{Prod}}} + T_{amb} \tag{1}$$

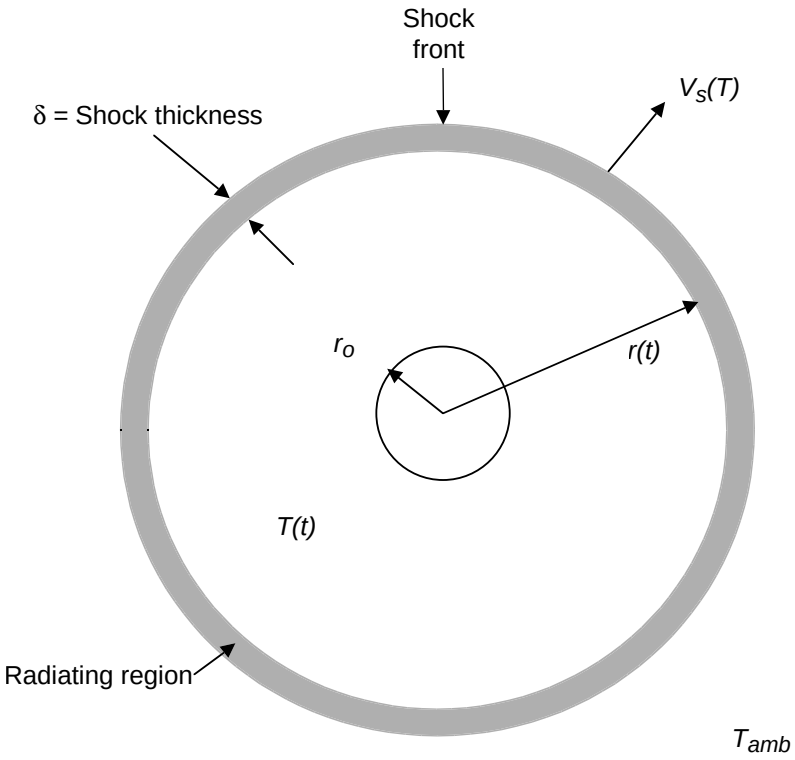


Figure 1. Idealized detonation model. (The undetonated charge occupies the spherical region of radius $r_0$. After completion of the detonation, a shock wave moves out with a velocity $V_s$. The thickness of the temperature discontinuity across the shock wave can be calculated by the formulas provided in the text.)

in which $T_{amb}$ = *300K (ambient temperature at sea level),* (2)

*and* $C_{V/det\ prod}$ *is the average heat capacity of the material inside the sphere of radius* $r_0$.

*For* $t > t_0$, *the shock wave spreads and the temperature of the enlarging spherical region bound by r(t) is determined by the heat capacity of the additional air as well as the detonation products: The energy, temperature, and pressure are distributed uniformly inside the spherical region behind the shock wave.*

*We assumed that the specific heat capacity of air is constant and equal to the mean value between specific heat capacity at the elevated density and pressure that exists behind the shock wave at* $t_0$ *and specific heat capacity at ambient pressure and temperature ahead of the shock wave*. This assumption greatly simplifies our estimate of the temperature rise inside the spherical shock region. The errors as large as a factor of 5 introduced by this assumption are negligible compared to errors of several orders of magnitude introduced by the temperature variation of the fraction of particles ionized, as we discuss later.

For $t > t_0$ and $r < r(t)$

$$T(t) = \frac{Q}{C_{V/air}(t) + C_{V/\det prod}} + T_{amb} \ , \qquad (3),$$

in which $C_{V/air}(t) = \left(\frac{4}{3}\pi\left(r^3(t) - r_0^3\right)\right)\rho_{amb}\, c_{Vs}$ . (4)

Here, $\rho_{amb}$ is the density of air at ambient temperature and pressure (1.23 kg/m$^3$) and $c_{Vs}$ is the constant-volume specific heat capacity of air at ambient temperature and pressure (717 J/kg-K).

The velocity of the shock wave as a function of temperature is calculated by Zel'dovich and Raizer [15]. The velocity of the shock wave can be described by their results, which we have fitted to the expression (see fig. 2):

$$V_s(t) = 5.5T^{0.76} \text{ m/s for } (293 \text{ K} < T < 15{,}000 \text{ K}) . \quad (5)$$

Once we know the initial velocity of the shock wave, $V_s(t_0)$, we can obtain the radius at the subsequent times by using the following equations:

$$r(t_i) = r(t_{i-1}) + V_s(t_{i-1}) \times (t_i - t_{i-1}) \quad (6)$$

in which

$t_i = t_{i-1} + \Delta t$ for $i \geq 1$

with $\Delta t = 10^{-6}$ s.

We must determine the value of $C_{v/det\ prod}$ in equation (3) as a function of temperature and pressure.

## 2.2 Temperature and Pressure Dependence of Heat Capacity of Detonation Products

Composition B explosive consists of 63 percent RDX, 36 percent Trinitrotoluene (dynamite) (TNT), and 1 percent paraffin filler. *The model assumes that the detonation takes place in a vacuum, i.e., in the absence of air. Thus, the program does not include further combustion of the detonation products in air.* The combustion product gases expand outward adiabatically after the completion of detonation. The detonation products of Composition B were obtained from the Cheetah computer program [16] that used the applicable chemistry. The detonation products obtained from the Cheetah model in concentrations greater than 1 mole of detonation product per kilogram of explosive are by weight, 24.1 percent $H_2O$, 36.4 percent $N_2$, 21.9 percent $CO_2$, 5.2 percent CO, and 12.1 percent solid carbon.

The specific heat capacity of the detonation product gases depends on temperature and pressure [17], [18]. Temperature dependence [17] is shown in figure 3. The total heat capacity, calculated from figure 3 and the relative concentrations, varies from 0.26 cal/gm-K at 300 K to 0.39 cal/gm-K at 3500 K. The pressure dependence is given in [17]. *The specific heat capacity of the*

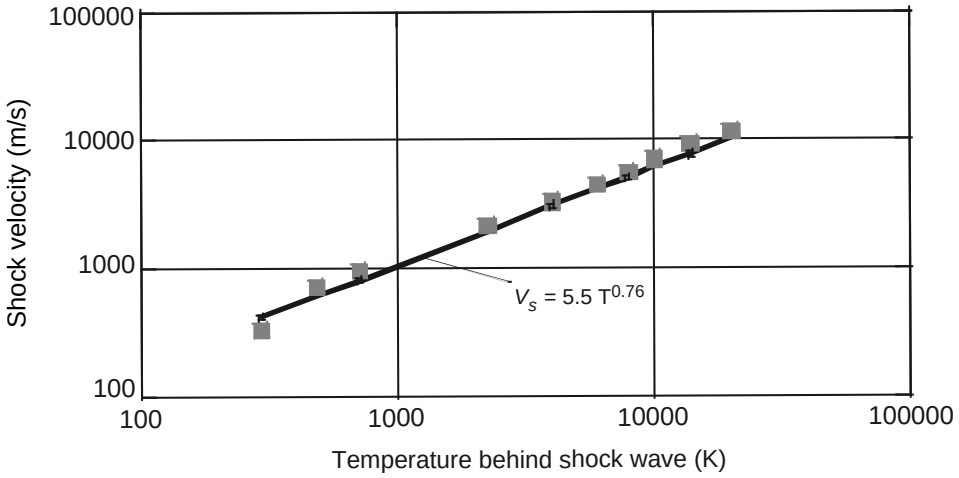


Figure 2. Shock wave velocity as a function of temperature behind the shock wave.

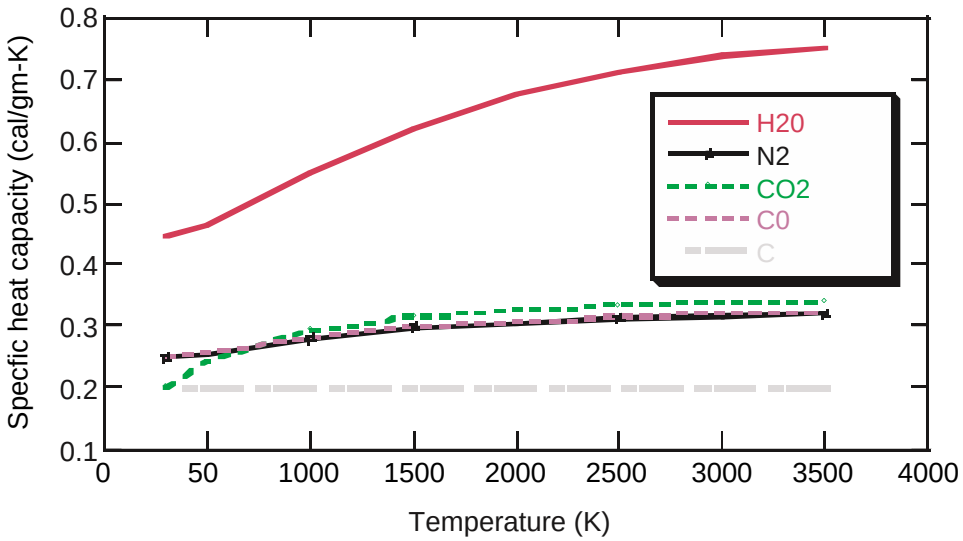


Figure 3. Temperature dependence of the specific heat capacity of the detonation products of Composition B. (The specific heat capacity of each of the five highest concentration detonation products of Composition B is shown.)

*detonation products varies adiabatically from 0.210 cal/gm-K at 1 atm to 0.587 cal/gm-k at 24 × 10⁴ atm. In the calculation, we use the mean value of 0.40 over these temperature and pressure ranges.*

The pressure and temperature variations on the specific heat capacity of air vary from 0.1719 cal/gm-K at 1 atm and 300 K to 0.315 cal/gm-K at 100 atm and 3000 K. *We use the mean value over this temperature and pressure range, 0.243 cal/gm-K.* This could result in values that are too large or too small by 30 percent over the pressure and temperature extremes.

These assumed values for the specific heat capacities of the detonation products and ambient air lead to errors that are negligible compared to the errors arising from the temperature dependence of the concentration of ionized particles.

## 2.3 Ionization Fraction

A previous report [2] showed that only a very small fraction of the particles are ionized. We therefore need a method that accounts for the ionization fraction of the radiation. The Hilsenrath and Klein calculation [19] of the ionization fraction of air as a function of temperature is shown in figure 4. One sees that the ionization fraction is very sensitive to changes in temperature below 15,000 K. We have interpolated the lower temperature ionization fraction results from Hilsenrath and Klein in figure 4. The interpolation formula is

$$Log_{10} IonizationFraction = Log_{10} f_i = \left(-30.566\right) + \left(0.011267\right) * T - \left(1.3664 \times 10^{-6}\right) * T^2 \quad (7)$$

Table 2 shows the ionization of various ion species in air at 3500 K and 2500 atmospheres [19] at the high temperatures and pressures that could occur during an explosion. Since air is composed primarily of $N_2$ and $O_2$, and since the dominant detonation products of Comp B explosive are $H_2O$, $N_2$, C, $O_2$, and $CO_2$, one might expect ionization fraction values of the same order of magnitude as air, which are calculated from equation 7 and plotted in figure 4. We see, however, that the tabulated results from table 2 are quite

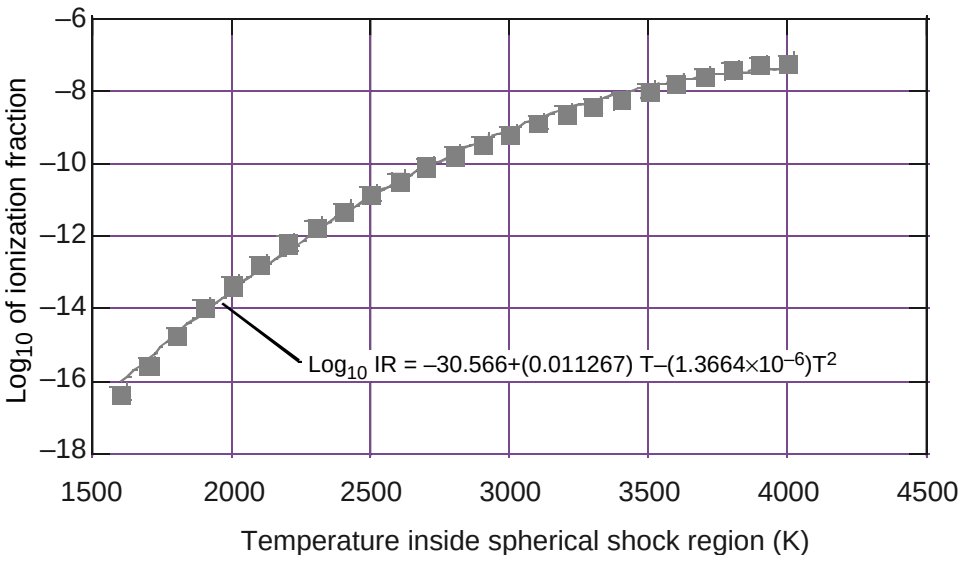


Figure 4. Curve fit to ionization fraction, IF, of air as a function of temperature. (The logarithm of the ionization fraction data from Reference 19 is plotted versus temperature of the air. The line obtained from the curve fit equation is also shown.)

Table 2. Ionization of air at 3500 K and 2500 atm.

| Species | Ionization fraction | Trend with increasing pressure |
|---|---|---|
| $NO^+$ | $3.1 \times 10^{-8}$ | decreasing |
| $O_2^+$ | $1.5 \times 10^{-11}$ | decreasing |
| $N_2^+$ | $2.3 \times 10^{-15}$ | decreasing |
| $O^+$ | $2.5 \times 10^{-15}$ | decreasing |
| $CO^+$ | $1.1 \times 10^{-17}$ | decreasing |
| $E^+$ | $1.0 \times 10^{-8}$ | decreasing |
| $O^+$ | $2.0 \times 10^{-8}$ | increasing |
| $C_2^+$ | $1.1 \times 10^{15}$ | increasing |

different from the values for air at 3500 K in figure 4. *Nevertheless, we assume that we can use equation 7 for determining the ionization fraction of the detonation products. We further assume that (a) the detonation products and the air are at most singly ionized, and that (b) the electron concentration, e–, is equal to the ion concentration.*

## 2.4 Radiation From Particle Acceleration Across a Shock Wave

Radiation is caused by the acceleration of charged particles because of the passage of the shock wave. Additional assumptions are as follow: *All the acceleration takes place over the thickness of the shock wave, which we shall show is on the order of $10^{-8}$ m. We apply the equipartition theorem [20] to provide a relationship for the mean particle speed V. Ideal gas behavior applies, and the air before and after the shock wave is in thermodynamic equilibrium.*

Since we are considering only the radial component of the electron's velocity, the problem is one-dimensional, with the result that the speed change, $\Delta V$, across the shock (neglecting direction changes) and the average speed across the shock, $\bar{V}$, as shown in figure 5, are given respectively by

$$\Delta V \approx V(t) - V\left(T_{amb}\right) = \sqrt{\frac{k}{m}}\left(\sqrt{T} - \sqrt{T_{amb}}\right) \ , \tag{8}$$

Figure 5. Change in mean speed of charged particles caused by temperature change across the shock wave for the one-dimensional case considered in the analysis.

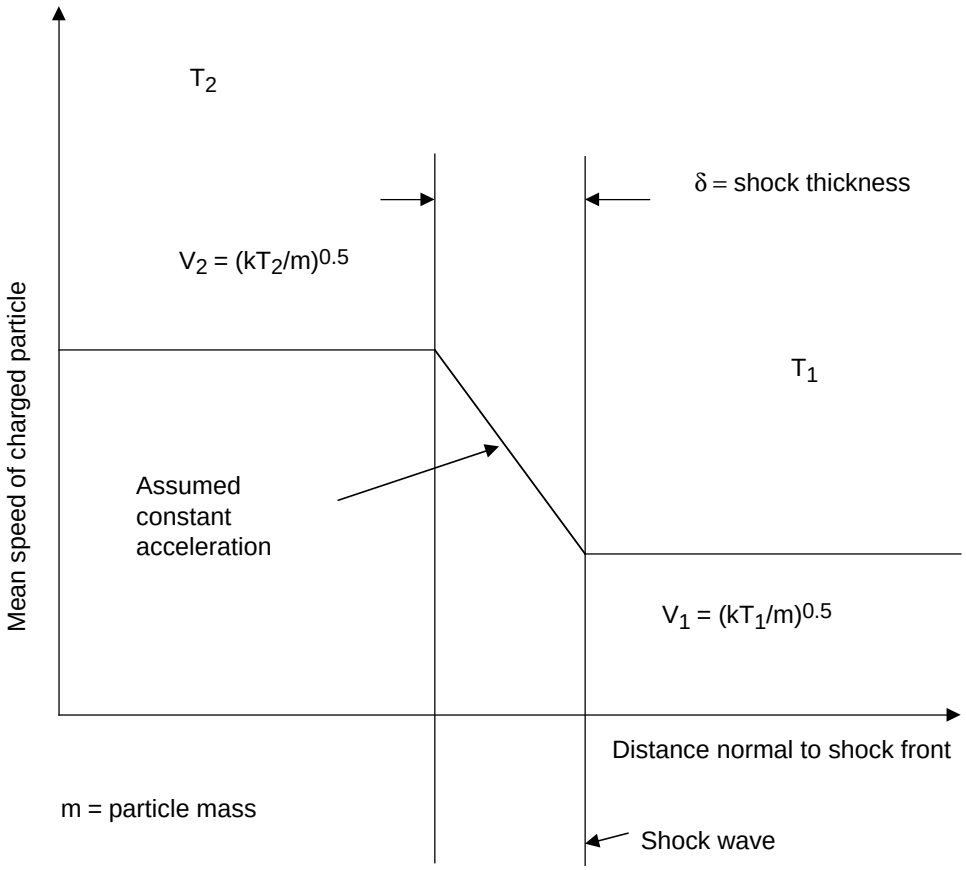


in which $k$ is the Boltzmann constant, $1.38 \times 10^{-23}$ J/K.

$$\bar{V} \approx \frac{V(T) + V\left(T_{amb}\right)}{2} = \sqrt{\frac{k}{m}} \frac{\left(\sqrt{T} + \sqrt{T_{amb}}\right)}{2} \ , \tag{9}$$

*in which V(T)* is the average radial velocity for $r > r_0$.

*The shock wave Mach number is defined by*

$$M(t) \equiv \frac{V_s(T(t))}{V_{\text{amb}}} \tag{10}$$

*in which $V_{amb}$, the speed of sound at ambient conditions, = 340 m/s.*

*The mean free path $\lambda$, which is the average distance that particles travel between collisions [21], is*

$$\lambda \approx \frac{16}{5} \frac{\nu}{\sqrt{2\pi R T_{amb}}} \tag{11}$$

*in which $\upsilon$ is the kinematic viscosity of air at ambient conditions ($14 \times 10^{-6}$ m$^2$/s) and R is the ideal gas constant of air (287 J/kg-K).*

*The shock thickness $\delta(t)$ is given by Kogan [21]*

$$\delta(t) \approx \frac{\gamma - 1}{\gamma + 1} M(t) \lambda \approx 10^{-8} M(t) \tag{12}$$

in which $\gamma$ is the ratio of the constant-pressure and constant-volume specific heat capacities of air, which we have assumed to be constant over the range of temperatures and pressures behind the shock.

The volume of air in the thin shock wave is

$$\tau_w = 4\pi r^2(t)\delta(t) \, . \tag{13}$$

*With the assumption of constant-volume and constant-density conditions,* the pressure rise produced is the bomb-yield energy divided by the volume of the spherical shock region, so that the pressure is

$$p(t) \approx p_{amb} + \frac{Q}{\frac{4}{3}\pi r^3(t)} \tag{14}$$

in which $p_{amb}$ is ambient pressure, $1.01 \times 10^5$ N/m$^2$.

During these conditions, the number of moles of air in the region in the shock wave is given by [22]

$$n(t) = \frac{p(t)\tau_w(t)}{RT(t)} \, . \tag{15}$$

Now consider a charged particle that accelerates with an acceleration *a(t)* across the shock front for a short time $\Delta t$ and continues moving in the same direction with the new velocity. The time of transit of the charged particle across the shock wave is

$$\Delta t \approx \frac{\delta}{\overline{V}} \tag{16}$$

and the acceleration of the charged particle is given by

$$a \approx \frac{\Delta V}{\Delta t} = \overline{V} \frac{\Delta V}{\delta} \, . \tag{17}$$

*We assume that the radiation is more or less uniformly distributed over a band starting at 0 Hz and extending to 1/*$\Delta t$ [23], given by

$$\Delta f \approx \frac{1}{\Delta t} \, . \tag{18},$$

and that from equation (17), we see that

$$\Delta f(t) \approx \frac{\overline{V}}{\delta(t)} \, . \tag{19}$$

*The time-average total power per singly ionized particle, P, integrated over all directions, is given by* [24]

$$P = \frac{e^2 a^2}{6\pi\varepsilon_0 c^3} = \frac{\mu_0 e^2 a^2}{c \quad 6\pi} \, , \tag{20}$$

in which $e$ is the electron charge ($1.6 \times 10^{-19}$ C); $\mu_0$, the permeability of free space (taken as equal to the permeability of air), is 1.26 μH/m; and $\varepsilon_0$, the permittivity of free space (taken as equal to the permittivity of air), is 8.85 pF/m.

The total power radiated for $n$ moles of singly ionized particles is

$$P_{total} \approx f_i nAP \,. \tag{21}$$

in which $A$ is the Avogadro's number, $6.02 \times 10^{23}$ particles/mole, and $f_i$ is the fraction of particles ionized from equation (7).

The average $E$-field per cycle produced in the far field per particle is given by [25]

$$E = \frac{1}{r}\sqrt{\frac{P\mu_0 c}{2\pi}} \tag{22}$$

Using equations 20, 21, and 22, we obtain the following formulas for the total $E$-field and $B$-field:

$$E_{total} \approx \left(\frac{1}{r}\right)\left(\sqrt{\frac{f_i(nA)\left(\frac{e^2 2a^2}{4\pi\varepsilon_0^3}\right)\mu_0 c}{2\pi}}\right) \approx \frac{\mu_0}{2\pi r}\frac{\sqrt{3}}{3}(ea)\sqrt{f_i na} \tag{23}$$

$$B_{total} \approx \frac{E_{total}}{c}\left(\mathrm{Wb/m^2}\right) \,. \tag{24}$$

Calculations have been performed for the case of an explosion having a yield that approximates the energy from a mortar projectile that is 25 MJ.

The calculated frequency bands shown in figure 6 include the observed frequency ranges of 6 to 250 MHz to 2 GHz, as shown in table 1. The electron frequency band is 1.4 THz, which is too high to be observed with RF, non-line-of-sight equipment. Figure 6 shows that the upper limits of the frequency bandwidths for $N_2$ and $O_2$ ions are about 8 to 9 GHz.

Figure 7 is the calculated $E$-field amplitude at a range of 10 km versus time from initiation of detonation for the $O_2$ ions, $N_2$ ions, and electrons. The $E$-field amplitude depends on the mass of the particles through the acceleration (eqs 17 and 23), the velocity change and average velocities (eqs 8 and

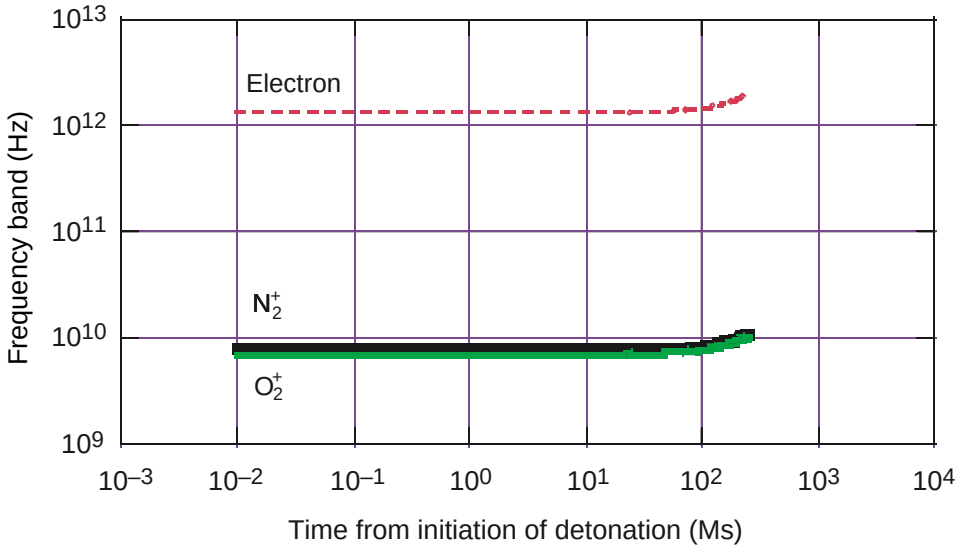


Figure 6. Calculated frequency band of radiation from electron, $O_2^+$, and $N_2^+$ ions formed when the shock wave from the detonation passes through ambient air. (The frequency band in volts/meter is plotted versus time in microseconds from initiation of detonation at 10 km.)

9). If equations (8) and (9) are substituted into equation (17), and the resulting acceleration is substituted into equation (23), the resulting expression shows that the *E*-field amplitude is inversely proportional to the masses of the particles. Thus, the radiation from the electrons should be more detectable than the radiation from the heavier $O_2^+$ and $N_2^+$.

If we arbitrarily assume that the detection threshold is $10^{-7}$ V/m, then from figure 7, the electron's radiation is detectable at 10 km for 100 μs, but the radiation from the $O_2^+$ and $N_2^+$ ions is not detectable. At 10 m from the explosion, the signal from the ions would increase to $2 \times 10^{-7}$ V/m, and would remain above the detection threshold for about 3 μs.

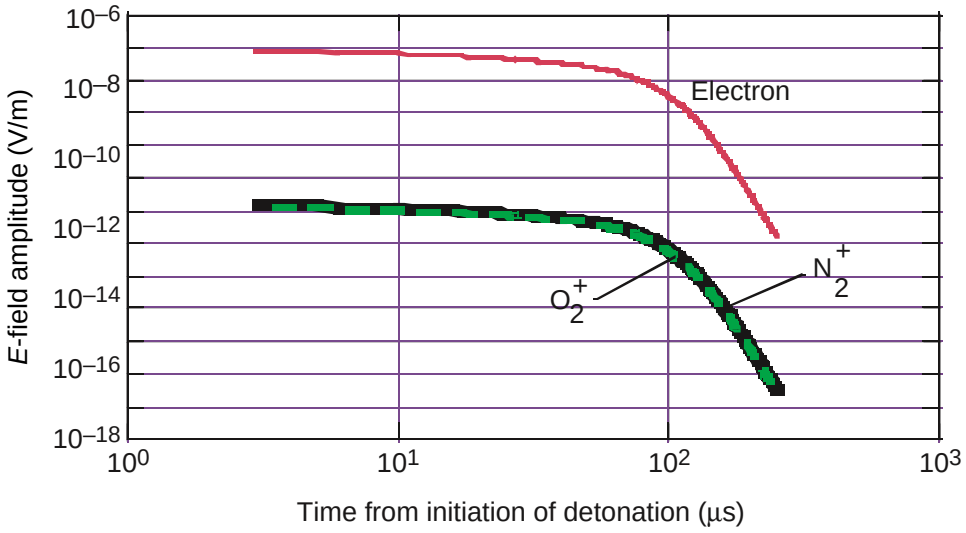


Figure 7. Calculated electric field amplitude of radiation from electron, $O_2^+$, and $N_2^+$ ions formed when the shock wave from the detonation passes through ambient air. (The *E*-field amplitude in volts/meter is plotted versus time in microseconds from initiation of the detonation at 10 km.)

# 3. Consequences of the Model

## 3.1 Effect of Explosive Mass

The model shows that the mass of the undetonated explosive affects both the amplitude of the radiation and the delay time from initiation of the explosion to completion of the detonation.

Equation (23) shows that the *E*-field amplitude is proportional to the square root of the number of moles of ionized particles, which *we assume is proportional to the mass of the undetonated explosive*. Thus, the model leads us to expect that the amplitude ratio should be proportional to the square root of the explosive mass.

The delay time from initiation to completion of the detonation is approximately the time for the detonation wave to propagate at constant velocity, $V_{det}$, from the center of the spherical explosive (point of initiation) to the surface of the explosive. From reference [3], the ratio of the delay times for two spherical explosives of uniform density but different masses should be proportional to the ratio of the cube roots of their masses.

## 3.2 Radiation From Recombination of Ions with Electrons

Heretofore, we have discussed the radiation caused by particles ionized during their passage through the shock region; we have not considered that the ions eventually re-combine with electrons, producing further radiation. Table 3 [26] gives the ionization energies and frequencies of the detonation products $N_2$ and $CO_2$.

The frequencies are in the terahertz region, with wavelengths in the ultraviolet spectrum, and therefore are not useful for transmission in non-line-of-sight scenarios.

## 3.3 Detectability of RF Signals From Detonation of Conventional Explosives

The detectability of the radiation depends on the thermal noise, background radiation noise, and the noise inherent in the sensor and data acquisition system. The examination of particular instrumentation systems and background radiation noise is beyond the scope of this report; however, we can make some general observations about the thermal noise. The thermal noise power is given by [27]

$$S_{noise} = kT_{amb}\Delta f \tag{25}$$

Table 3. Radiation from recombination of detonation products.

| Detonation product | Ionization energy (e-V) | Ionization energy (J) | Frequency (Hz) | Wavelength (Å) |
|---|---|---|---|---|
| $N_2$ | 15.5 | $2.48 \times 10^{-18}$ | $3.73 \times 10^{15}$ | 800 |
| $CO_2$ | 14.4 | $2.30 \times 10^{-18}$ | $4.0 \times 10^{15}$ | 750 |

in which $T_{amb}$ is the absolute temperature of the circuits in K, here taken to be 300 K, and $\Delta f$ is the frequency bandwidth of the signal in hertz. The calculated values of $\Delta f$ and $E$ from figures 6 and 7 are given in table 4, with the noise power calculated from equation (25).

The power $P_{avg}$ received by a 1-m$^2$ antenna far from the source can be estimated from the plane wave relationship [28], via $E$-field values obtained from figure 7:

$$P_{avg}(watts) = \left[\frac{1}{2} c\varepsilon_0 E_{peak}^2\right] A_{eff}\left(m^2\right) = \left[0.00133 E_{peak}^2\right] A_{eff} \ , \tag{26}$$

$c$ and $\varepsilon_0$ were defined previously.

Table 4 shows that the average power received is far less than the $kT\Delta f$ noise as close as 1 m to the detonation. The electron, which is the most detectable particle, is 11 dB below the noise, even at 1 m, and is 91 dB below noise at 10 km. Even if an explosive 10,000 times larger than the mortar (equivalent to a 4000-lb bomb) is used, only the electron radiation is detectable above the noise at close distances.

Using $E$-field amplitudes and frequency bands from figures 6 and 7, we can calculate the signal level relative to the noise at 1 m and 10 km from the detonation. The data are then extrapolated to an explosive having 10,000 times more mass.

These calculations have shown that the wide-band signals can be expected from radiation caused by ionized particles accelerating across the shock wave; however, the signals are not detectable above $kT\Delta f$ noise for normal sized explosives at useful detection ranges. Thus, the assumptions have oversimplified the phenomenon, or the model has not established the mechanism responsible for the signals measured by previous investigators (see table 1 and sect. 2).

Table 4. Detectability of estimated radiation from shock wave.

| Particle | Calculated $E$-field (V/m) | $\Delta f$ (Hz) | Noise power (W) | Calculated Average power at receiver (W) | Detectability (dB) |
|---|---|---|---|---|---|
| **0.191 kg explosive (mortar)** | | | | | |
| | | | **At 1 m** | | |
| Electron | $6 \times 10^{-4}$ | $1.6 \times 10^{12}$ | $6 \times 10^{-9}$ | $4.8 \times 10^{-10}$ | –11 |
| $N_2$ Ion | $1 \times 10^{-8}$ | $9 \times 10^{9}$ | $3.7 \times 10^{-11}$ | $1.3 \times 10^{-19}$ | –84 |
| $O_2$ Ion | $9 \times 10^{-9}$ | $8 \times 10^{9}$ | $3.3 \times 10^{-11}$ | $1.07 \times 10^{-19}$ | –85 |
| | | | **At 10 km** | | |
| Electron | $6 \times 10^{-8}$ | $1.6 \times 10^{12}$ | $6 \times 10^{-9}$ | $4.8 \times 10^{-18}$ | –91 |
| $N_2$ Ion | $1 \times 10^{-12}$ | $9 \times 10^{9}$ | $3.7 \times 10^{-11}$ | $1.3 \times 10^{-27}$ | –164 |
| $O_2$ Ion | $9 \times 10^{-13}$ | $8 \times 10^{9}$ | $3.3 \times 10^{-11}$ | $1.07 \times 10^{-27}$ | –165 |

## 3.4 Discussion

The calculations and order-of-magnitude model address the radiation produced by explosions that occur in bomb and projectile detonations. The bare explosive (not the explosive encased by the bomb or projectile shell) is considered. The mechanism of radiation analyzed was radiation from particles ionized by passage of the shock wave. The most common charged particles from the atmosphere are the $O_2^+$ ions and $N_2^+$ ions and the electrons. The calculations that were presented for each type of particle are the radiation bandwidth, time-average *E*-field and *B*-field amplitudes.

The values of bandwidth measured by experimeters (see table 1) ranged from 1 MHz to 1 GHz. The values from the model extend from 8 GHz for the ions to terahertz for the electrons.

The heat capacity of the detonation products and of the ambient air determine the temperature of the region of high temperature, pressure, and density behind the shock wave. The concentration of ionized particles strongly depends on the temperature behind the spherical shock wave. It decreases very steeply as the temperature drops during the shock wave expansion. An estimate was made of the dependence of the ion concentration on temperature. Relationships were established between explosive mass of uncased Composition B, the radiation frequency bands, and the *E*- and *B*-field amplitudes as a function of detection distance. At a range of 10 km, radiation from free electrons caused by a mortar-sized blast is expected in the frequency band up to 1.6 THz with amplitudes above 0.01 microvolt/m for the first 100 μs from detonation. Oxygen and nitrogen ions produce radiation in the frequency band up to 9 GHz with amplitudes above 10 picovolt/m for 3 μs after detonation.

A comparison of the calculated radiation with thermal noise estimates shows that most of the radiation is not detectable above the noise even for large explosives at close distances. The fact that signals have been observed suggests either that the assumptions over-simplify the phenomenon or that the radiation detected must be caused by other mechanisms.

The times for the ions and electrons to cross the shock wave are the reciprocals of the frequency bands from figure 6: $10^{-10}$ s for the ions and $10^{-12}$ s for the electrons. The particles exist in the charged state for the duration of the explosive event, which from figures 6 and 7, is nominally 100 μs or $10^{-4}$ s. This is $10^6$ times longer than the shock transit time for the ions and $10^8$ times longer for the electrons. During this much longer time, the charged particles could be producing radiation by some other mechanism. We therefore believe that the model greatly underestimates the quantity of radiation produced.

## Acknowledgment

The author acknowledges the efforts of Dr. Alan Edelstein of ARL whose painstaking technical review and many suggestions contributed greatly to the quality and utility of this report.

## References


1. Fine, J., and S. J. Vinci, "Causes of Electromagnetic Radiation From Conventional Explosives," 1997 Sensors and Electron Devices Symposium, University of Maryland, College Park, MD (14–15 January 1997).
2. Hull, D. M., and J. E. Fine, "Possible Upset Mechanisms of the PAM FTC Fuze Related to Explosively Generated Electric Charges: A Preliminary Study," Washington, DC, Army Research Laboratory Report ARL-MR-373 (March 1998), pp 7–8.
3. Fine, J. E., and S. J. Vinci. "Causes of Electromagnetic Radiation From Detonation of Conventional Explosives: A Literature Survey," Army Research Laboratory Report ARL-TR-1690 (December 1998), pp 9–10.
4. Trinks, H., *Electrical Charge and Radiation Effects near Projectiles and Fragments*, unpublished Harry Diamond Laboratories report (September 1976).
5. Takakura, T., *Publ. Astron. Soc. Jpn* **7**, No. 4, 210–220 (August 1955).
6. Stuart, W., *Data Interpretation for Hostile Weapons Location Program Vol. IV: Electromagnetic Emissions from Weapons and Explosions (U)*, Battelle Memorial Institute, ESD-TA-75-221, June 1975. (Formerly SECRET version downgraded to UNCLASSIFIED, March 27, 1998)
7. Curtis, G. D., "ELF Electromagnetic Radiation from Small Explosive Charges in Air and Water," Proceedings of the Institute of Radio Engineers (IRE) (November 1962), pp 2298–2301.
8. Gorshunov, L. M., G. F. Kononenko, and E. I. Sirotonin, "Electromagnetic Disturbances Accompanying Explosions," Soviet Physics JEPT, Vol. 26, No. 3 (March 1966), pp 500–502.
9. Cook, Melvin A., *The Science of High Explosives*, New York, Reinhold Publishing Corporation (1958), pp 159–171.
10. Wouters, L. F., "Implications of EMP from HE Detonation," Symposium Proceedings, AFSWC Symposium, Albuquerque, New Mexico, 12-13 March 1979. UCRS-72149/Prepring Lawrence Radiation Laboratory, University of California, Livermore, CA (15 January 1970).
11. van Lint, V.A.J., "Electromagnetic Emission From Chemical Explosions," IEEE Transactions on Nuclear Science, Vol. NS-29, No. 6 (December 1982).
12. Anderson, W. H., and C. L. Long, "Electromagnetic Radiation from Detonating Solid Explosives," J. Appl. Phys., Vol. 36, No. 4 (April 1965), pp 1494–1495.
13. Baker, W., *Explosions in Air*. Austin, TX, University of Texas Press (1973), Chapter 1.
14. Bailey. A., and S. G. Murray, *Explosives*, *Propellants*, *and Pyrotechnics*, *Vol 2*, Brassey's New Battlefield Weapons Systems and Technology Series, BPCC Wheatons Ltd., Exeter (1989), p. 34.

15. Zel'dovich, Ya. B., and Yu. P. Raizer, *Physics of Shock Waves and High-Temperature Hydrodynamic Phenomena*, Vol I & Vol II, New York, Academic Press (1967), p 212.

16. Reaugh, J., *Cheetah Calculations for Comp B*, Energetic Materials Center, Lawrence Livermore National Laboratory, Livermore, CA (23 January 1998).

17. Van Wylen, G. J., and R. E. Sonntag, *Foundations of Classical Thermodynamics*, New York: John Wiley & Sons, 1973, Table A.9 "Constant-Pressure Specific Heats of Various Ideal Gases."

18. Hilsenrath, J., C. W. Beckett, W. S. Benedict, L. Fano, H. J. Hoge, J. F. Masi, R. L. Nuttall, Y. S. Touloukian, and H. W. Woolley, *Tables of Thermal Properties of Gases*, Washington, D.C., National Bureau of Standards Circular 564, issued November 1, 1955, Table 2–3, "Specific Heat of Air."

19. Hilsenrath, J., and M. Klein, *Tables of Thermodynamic Properties of Air in Chemical Equilibrium Including Second Virial Corrections from 1500 to 15,000 K*, Arnold Engineering Development Center, Tullahoma, TN, Technical Report AEDC-TR-65-68 (March 1965)

20. Reif, F., *Statistical Physics* (Berkeley Physics Course, Vol 5), New York, McGraw-Hill Book Co. (1965), pp 248–249.

21. Kogan, M. N., *Rarefied Gas Dynamics*, New York, Plenum Press (1969), pp 347, 341, eq 4.20.

22. Alberty, R. A., and R. J. Silbey, *Physical Chemistry* (first edition), New York, John Wiley & Sons Inc. (1992), p 9.

23. Panter, P. F., *Modulation*, *Noise*, *and Spectral Analysis*, New York, McGraw-Hill Book Company (1965), p 41.

24. Eisberg, R. Eisberg, and L. Lerner, *Physics Foundations and Applications*, New York, McGraw-Hill (1981), pp 1295–1308.

25. Halliday, D., and R. Resnick, *Physics for Students of Science and Engineering*, Vol II, Edition I, New York, John Wiley & Sons, Inc. (1962), p 897.

26. Sedlacek, M., *Electron Physics of Vacuum and Gaseous Devices*, New York, John Wiley and Sons, Inc. (1966), pp 388–389.

27. Skolnik M., Editor-in-Chief, *Radar Handbook*, *Edition II*, New York, McGraw-Hill, Inc. (1990), p. 17.

28. Lorrain, P., and D. Corson, *Electromagnetic fields and Waves*, San Francisco, W. H. Freeman and company, 1970, p. 465.

# Distribution

Admnstr
Defns Techl Info Ctr
ATTN DTIC-OCP
8725 John J Kingman Rd Ste 0944
FT Belvoir VA 22060-6218

DARPA
ATTN D Cress
ATTN S Welby
3701 N Fairfax Dr
Arlington VA 22203-1714

Defns Threat Reduction Agcy (DTRA)
ATTN CSOB K Calahan
ATTN CPFO/ATC W Brown
ATTN CPA S E Dains
6801 Telegraph Rd
Alexandria VA 22310-3398

Defns Threat Reduction Agency
ATTN SWP-1 E Rinehart
ATTN SWTI A Verna
ATTN SWTI G Lu
1680 Texas Stret, SE
Kirtland AFB NM 87117-5669

Ofc of the Secy of Defns
ATTN ODDRE (R&AT)
The Pentagon
Washington DC 20301-3080

PEO-Theater Air Defns Natl Ctr
ATTN 2/9W62 D Marker, Technology Dir
2531 Jefferson Davis Highway
Arlington VA 22242-5170

AMCOM MRDEC
ATTN AMSMI-RD W C McCorkle
Redstone Arsenal AL 35898-5240

US Army TRADOC
Battle Lab Integration & Techl Dirctrt
ATTN ATCD-B
FT Monroe VA 23651-5850

Dir for MANPRINT
Ofc of the Deputy Chief of Staff for Prsnnl
ATTN J Hiller
The Pentagon Rm 2C733
Washington DC 20301-0300

Ofc of the Proj Mgr for Mines, Countermines, & Demltn
ATTN AMCPM-DSA-MCD T Hoffman
ATTN AMCPM-TDS-MC R Andrejkovics
Picatinny Arsenal NJ 07806-5000

SMC/CZA
2435 Vela Way Ste 1613
El Segundo CA 90245-5500

US Army ARDEC
ATTN AMSTA-AR-TD
Bldg 1
Picatinny Arsenal NJ 07806-5000

US Army Info Sys Engrg Cmnd
ATTN AMSEL-IE-TD F Jenia
FT Huachuca AZ 85613-5300

US Army Natick RDEC Acting Techl Dir
ATTN SBCN-T P Brandler
Natick MA 01760-5002

US Army Simulation Train & Instrmntn Cmnd
ATTN AMSTI-CG M Macedonia
ATTN J Stahl
12350 Research Parkway
Orlando FL 32826-3726

US Army Spc & Strtgc Defns Cmnd
ATTN CSSD-TC-ST K Blankenship
PO Box 1500
Huntsville AL 35807-3801

US Army Tank-Automtv Cmnd RDEC
ATTN AMSTA-TR J Chapin
Warren MI 48397-5000

Commander-in-Chief
Atlantic Fleet
ATTN Code N-8 R Whiteway
1562 Mitscher Ave
Norfolk VA 23551

Nav Air Warfare Ctr Unconventional Observables/Techl Oversight Ofc
ATTN Code 526E00D D Schriner
China Lake CA 93555-6001

## Distribution (cont'd)

Nav Air Warfare Ctr Weapons Div
ATTN Code 474330D H John, Jr.
ATTN T M Atienza-Moore
China Lake CA 93555-6001

Nav Rsrch Lab
ATTN Code 6650 T Wieting
4555 Overlook Ave SW
Washington DC 20375-5000

Nav Surfc Warfare Ctr
ATTN Code B07 J Pennella
17320 Dahlgren Rd Bldg 1470 Rm 1101
Dahlgren VA 22448-5100

Lawrence Livermore Natl Lab
ATTN L228 J Morrison
ATTN L282 J Reaugh
ATTN L282 M Murphy
PO Box 808
Livermore CA 94551-5554

Los Alamos Natl Lab
ATTN DARHT E Pogue
MAIL STOP P941
Los Alamos NM 87545

Los Alamos Natl Lab
ATTN DOD K F McKenna
Mail Stop F613
Los Alamos NM 87545

Los Alamos Natl Lab
ATTN DX3 L Hull
Mail Stop P940
Los Alamos NM 87545

Los Alamos Natl Lab
ATTN NW/CWT J V Repa
Mail Stop F613
Los Alamos NM 87545

Los Alamos Natl Lab
ATTN P22 R E Kelly
Mail Stop D410
Los Alamos NM 87545

Hicks & Assoc Inc
ATTN G Singley III
1710 Goodrich Dr Ste 1300
McLean VA 22102

Lab for Physical Sciences
ATTN A J Leyendecker, PH.D.
Senior Scientist
8050 Greenmead Dr
College Park MD 20740

Palisades Inst for Rsrch Svc Inc
ATTN E Carr
1745 Jefferson Davis Hwy Ste 500
Arlington VA 22202-3402

Director
US Army Rsrch Lab
ATTN AMSRL-RO-D JCI Chang
PO Box 12211
Research Triangle Park NC 27709

US Army Rsrch Lab
ATTN AMSRL-CI-IS-R Mail & Records Mgmt
ATTN AMSRL-CI-IS-T Techl Pub (2 copies)
ATTN AMSRL-CI-OK-TL Techl Lib (2 copies)
ATTN AMSRL-DD J M Miller
ATTN AMSRL-SE H Leupold
ATTN AMSRL-SE J Pellegrino
ATTN AMSRL-SE-DP M Litz
ATTN AMSRL-SE-DS J Miletta
ATTN AMSRL-SE-DS L Jasper
ATTN AMSRL-SE-R A Sindoris
ATTN AMSRL-SE-RE R Chase
ATTN AMSRL-SE-RU B Scheiner
ATTN AMSRL-SE-RU M Ressler
ATTN AMSRL-SE-SA J Eicke
ATTN AMSRL-SE-SS A Edelstein
ATTN AMSRL-SE-SS D Hull
ATTN AMSRL-SE-SS G Fischer
ATTN AMSRL-SE-SS J Chopack
ATTN AMSRL-SE-SS J Fine (20 copies)
ATTN AMSRL-SE-SS J Hopkins
ATTN AMSRL-SE-SS M Kolodny
ATTN AMSRL-SE-SS S Vinci
ATTN AMSRL-SE-SS V Marinelli
Adelphi MD 20783-1197

# REPORT DOCUMENTATION PAGE

*Form Approved*
*OMB No. 0704-0188*



| 1. AGENCY USE ONLY *(Leave blank)* | 2. REPORT DATE | 3. REPORT TYPE AND DATES COVERED |
|---|---|---|
| | September 2001 | Final, December 1995 to 1998 |

**4. TITLE AND SUBTITLE** Estimates of the Electromagnetic Radiation From Detonation of Conventional Explosives

**5. FUNDING NUMBERS**
DA PR: AH-16
PE: 62120A

**6. AUTHOR(S)** Jonathan E. Fine

**7. PERFORMING ORGANIZATION NAME(S) AND ADDRESS(ES)**
U.S. Army Research Laboratory
Attn: AMSRL-SE-SS email: jfine@arl.army.mil
2800 Powder Mill Road
Adelphi, MD 20783-1197

**8. PERFORMING ORGANIZATION REPORT NUMBER**
ARL-TR-2447

**9. SPONSORING/MONITORING AGENCY NAME(S) AND ADDRESS(ES)**
U.S. Army Research Laboratory
2800 Powder Mill Road
Adelphi, MD 20783-1197

**10. SPONSORING/MONITORING AGENCY REPORT NUMBER**

**11. SUPPLEMENTARY NOTES**
ARL PR: 7NE4TR
AMS code: 622120.H16

**12a. DISTRIBUTION/AVAILABILITY STATEMENT** Approved for public release; distribution unlimited.

**12b. DISTRIBUTION CODE**

**13. ABSTRACT** *(Maximum 200 words)*

An order of magnitude model is presented to estimate radiation from detonation of conventional explosives in an attempt to predict frequency bands and signal levels detected by other investigators. An earlier model describing the radiation generated by explosions has been refined to include the contribution of the heat capacity of the detonation products and the temperature dependence of the concentration of ionized particles. Relationships are established between explosions of uncased Composition B, the radiation frequency bands, and the *E*- and *B*-field amplitudes as a function of detection distance. The model considers the radiation from particles ionized by passage of the shock wave.

A comparison of the calculated radiation with thermal and background noise estimates shows that the radiation is not detectable above the background radiation even for large explosives at close distances. The fact that radiation has been observed indicates either that the assumptions over-simplify the phenomenon or that the primary mechanism of radiation production has been overlooked. Ionized particles exist $10^6$ to $10^8$ times longer than the time to accelerate across the shock wave, during which the particles could produce radiation by some other means. Therefore, it is likely that the model greatly underestimates the quantity of radiation produced.

**14. SUBJECT TERMS** Explosion sensor, rf from explosions, rf signature, shock wave radiation, detonation radiation, explosion signature, projectile detonation varification, missile launch verification, artillery rf signature

**15. NUMBER OF PAGES**
26

**16. PRICE CODE**

| 17. SECURITY CLASSIFICATION OF REPORT | 18. SECURITY CLASSIFICATION OF THIS PAGE | 19. SECURITY CLASSIFICATION OF ABSTRACT | 20. LIMITATION OF ABSTRACT |
|---|---|---|---|
| Unclassified | Unclassified | Unclassified | UL |

NSN 7540-01-280-5500

Standard Form 298 (Rev. 2-89)
Prescribed by ANSI Std. Z39-18
298-102